10th International Conference on Indium Phosphide and Related Materials
May 11-15, 1998

POWER PERFORMANCE OF PNP InAlAs/InGaAs HBTs

D. Sawdai, X. Zhang, D. Pavlidis, and P. Bhattacharya

Solid-State Electronics Laboratory, Department of Electrical Engineering and Computer Science
The University of Michigan, Ann Arbor, Michigan 48109, U.S.A.
http://www.eecs.umich.edu/dp-group/

Abstract

Recently, small-signal microwave performance has been reported for PNP InAlAs/InGaAs HBTs [1, 2]. While power performance of PNP AlGaAs/GaAs HBTs has been demonstrated [3], nothing has been reported on power performance of PNP HBTs in the InP material system. In this work, InAlAs/InGaAs PNP HBTs were fabricated and subsequently characterized under large signal conditions at X-band to determine their suitability for high-frequency power applications. PNP HBTs demonstrated f_T and f_{max} as high as 13 and 35 GHz, respectively. Power performance at 10 GHz was comparable to InP-based NPN single HBTs, providing up to 10 dB of gain, 0.49 mW/μm^2 of output power, and 24% power-added efficiency. Analysis of these HBTs suggests further design and epilayer optimizations for increased power performance.

I. Introduction

InP-based HBTs have demonstrated excellent frequency performance and extremely good current-handling capability. Research on InP-based HBTs has almost exclusively focused on NPN HBTs, since the electron velocity is several orders of magnitude higher than the hole velocity in InGaAs. PNP HBTs are also of interest, primarily for integration in circuits with NPN HBTs. Together, NPN and PNP HBTs can form a simple, efficient, and linear Class B power amplifier or output buffer. Such an AlGaAs/GaAs integrated NPN/PNP push-pull amplifier has demonstrated power performance at 2.5 GHz [4]. Multiple-stage amplifiers could be designed with alternating NPN and PNP stages, allowing for simple designs with a single power supply and direct coupling between stages. PNP HBTs could also be used as active loads and current sources for NPN amplifier stages, which would provide higher gain per stage, reduced power consumption in the load, and reduced wafer area consumed by passive resistors. Overall, the integration of PNP with NPN HBTs offers simpler circuits with fewer components and reduced power consumption.

While not as impressive as their NPN counterparts, the current state-of-the-art frequency performance for PNP HBTs are sufficient for X-band and higher performance. The best-published InAlAs/InGaAs PNP HBTs demonstrated $\beta = 170$, $f_T = 14$ GHz, and $f_{max} = 22$ GHz [2], while the best published InP/InGaAs PNP HBTs demonstrated $\beta = 20$, $f_T = 11$ GHz, and $f_{max} = 25$ GHz [5]. In the AlGaAs/GaAs material system, results have been presented with $\beta = 11$, $f_T = 33$ GHz, and $f_{max} = 66$ GHz [6]. The apparent higher performance of the GaAs-based HBTs is mostly due to more aggressive base designs and higher attainable doping in the emitter cap and subcollector.

II. Device Design and Fabrication

Two sets of PNP epilayers were grown on Fe-doped semi-insulating (001) InP by solid-source molecular beam epitaxy at The University of Michigan. The growth rate was 0.7 μm/h at 490° C, and an InGaAs/InAlAs superlattice was grown on the substrate to improve the material quality. The background doping for undoped InGaAs layers was below 5×10^{15} cm^{-3}, and undoped InAlAs layers were semi-insulating.

Both layer structures were almost identical [1] except for the doping of the 500-Å base layer: Wafer A had a uniform 5×10^{18} cm^{-3} base doping, which resulted in a sheet resistance of 76 Ω/❑ and a contact resistivity to Ti/Pt/Au of 1.0×10^{-6} Ω-cm^2. Wafer B had a linearly-graded base doping from 5×10^{18} cm^{-3} at the emitter end to 1×10^{18} cm^{-3} at the collector end, which resulted in a sheet resistance of 165 Ω/❑ and a contact resistivity to Ti/Pt/Au of 1.9×10^{-6} Ω-cm^2. Both wafers were fabricated with the same process, which was based upon a high-performance NPN HBT process described elsewhere [7]. Nominal HBT emitter dimensions varied from 1-finger 1×10 μm^2 to 10-finger 5×40 μm^2, with typical dimensions of 2×10 μm^2 and 5×10 μm^2.

III. DC and Small-Signal Microwave Results

The DC characteristics of Wafer A are described in detail elsewhere [1]. For a 5×10 μm^2 HBT, the breakdown voltage BV_{ECO} (at 10 A/cm^2) was 5.6 V. From the Gummel plot, the ideality factors n_B and n_C were 1.60 and 1.00, respectively, and the maximum β was 12 at $J_C = 34.8$ kA/cm^2. The gain increased significantly ($\beta > 20$ and $h_{fe} > 30$) at higher V_{EC}. However, the gain compressed rapidly for $J_C > 50$ kA/cm^2,

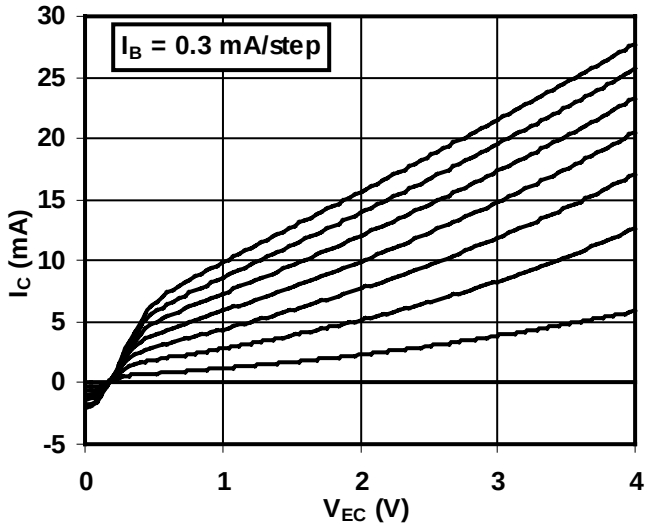

Fig. 1: Forward I-V characteristics of 5×10 μm² HBT from Wafer B. I_B = 0.3 mA/step.

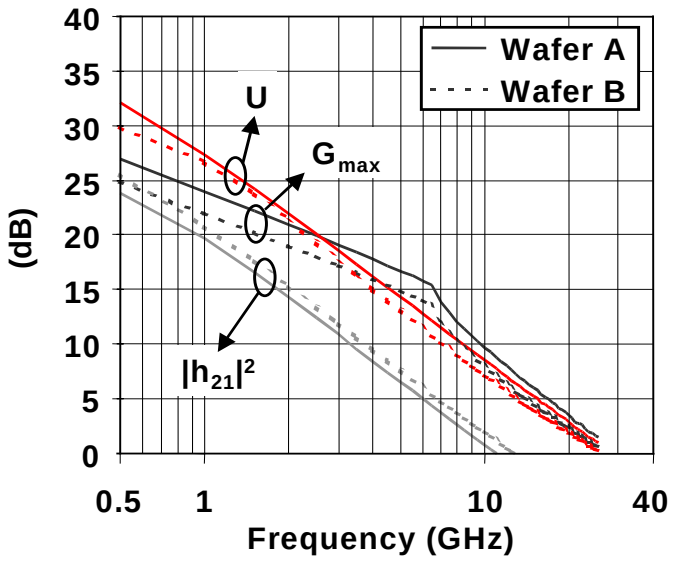

Fig. 2: Frequency response of 5×10 μm² HBTs from Wafers A and B

which was attributed to base push-out through simulations using similar collector doping.

Both $|h_{21}|^2$ and G_{max} were calculated from on-wafer common-emitter measurements of the S-parameters up to 25.5 GHz and extrapolated (when necessary) at 20 dB/decade to find f_T and f_{max}, respectively. The optimal frequency performance was f_T = 11 GHz and f_{max} = 31 GHz at V_{EC} = 4.0 V and I_C = 11.69 mA. Due to the short diffusion length of the holes, base push-out had a very significant effect on both gain and high-frequency performance at higher current densities. At similar bias conditions for a 1×10 μm² HBT from Wafer A, the best frequency performance was f_T = 12 GHz and f_{max} = 35 GHz. This is the highest reported f_{max} for any InP-based PNP HBT.

The characteristics of the 5×10 μm² HBT on Wafer B (see Fig. 1) were very similar to those on wafer A. The breakdown voltage BV_{ECO} (at 10 A/cm²) was 6.8 V, and the maximum β with V_{BC} = 0 V was 4.2 at J_C = 14.2 kA/cm². Similar to Wafer A, the gain increased significantly ($\beta > 20$) at higher V_{EC}.; however, the Early effect was more pronounced for Wafer B due to the lower base doping near the collector. The best frequency performance was f_T = 13 GHz and f_{max} = 26 GHz at V_{EC} = 4.5 V and I_C = 6.47 mA (see Fig. 2). Comparing to Wafer A, the 15% increase in f_T is due to a 25% decrease in τ_b caused by the drift electric field in the base. However, the lower average doping in the graded profile that created this drift field also increased R_B by 85%, resulting in a 13% decrease in f_{max}.

IV. Power Characterization

On-wafer power characterization was performed at 10 GHz using a system developed in-house using FOCUS electromechanical tuners on both the source and the load. The 5×10 μm² HBT from Wafer A was biased using constant V_{EB} and V_{EC} while the source and load impedances were optimized for maximum gain at P_{in} = -20 dBm, resulting in Γ_S = 0.740∠-179° and Γ_L = 0.596∠26°. The power characteristics at these impedances (Fig. 3) demonstrate a small-signal gain of 10.0 dBm, peak power-added efficiency of 24%, and a maximum output power density of 0.49 mW/μm². These characteristics are very similar to InP-based NPN single HBTs fabricated with the same technology [8]: the NPN HBTs showed slightly higher gain (+1 dB) and efficiency (+5%), while the PNP HBTs produced more output power (+3 dBm) before saturating. Note that these NPN HBTs, which provide up to 1.37 mW/μm², show the best reported power performance for InP-based NPN single HBTs and are only surpassed by double HBTs, which provide up to 3.6 mW/μm² [9]. While power handling capability has not previously been reported for InP-based PNP HBTs, GaAs-based PNP HBTs have demonstrated output power up to 0.63 mW/μm² [3], which is comparable to the HBTs presented in this work.

Load-pull characteristics of the PNP HBT at P_{in} = 3.17 dBm and at 1-dB of gain compression demonstrated that the optimal load impedances for linearity, gain, and efficiency are approximately the same, indicating that circuit designs need not choose impedances to trade off these characteristics. In contrast, previous studies of NPN HBTs [8] demonstrated that any single load impedance either reduces the gain by 4 dB, the maximum output power by 2 dB, or the efficiency by 14 % from the best-matched values.

Several power studies were performed at 10 GHz on the HBTs from both wafers to determine the influence of layer structure, emitter geometry, number of emitter fingers, and common-emitter versus common base configuration. All HBTs were biased under approximately the same conditions: constant V_{EC} = 4.00 V (for common base, V_{BC} = 3.20 V since $V_{EB} \approx$ 0.8 V), constant V_{EB} adjusted for maximum small-signal microwave gain, and Γ_S and Γ_L optimized for maximum small-signal microwave gain. The only exception is one set of data which was taken at V_{BC} = 4.00 V for a common-base 2-finger

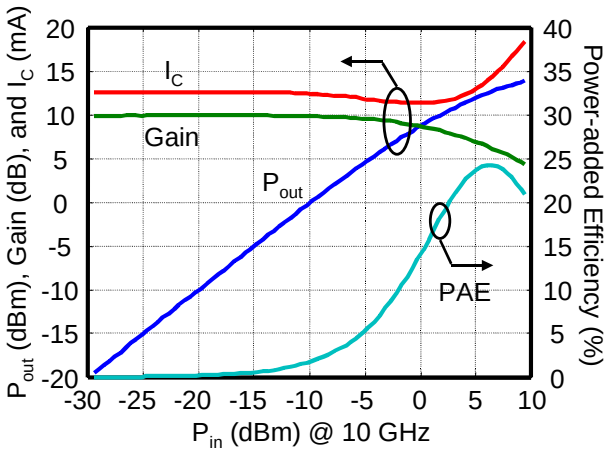

Fig. 3: Power characteristics of 5×10 μm² HBT from Wafer A under constant V_{EB} bias with V_{EC} = 4.0 V. Maximum P_{out} = 0.49 mW/μm² and PAE = 24%.

5×10 μm² HBT. Some of the resulting data is shown in Fig. 4, where the curves connect HBTs of the same emitter geometry but with 1, 2, 4, or 10 emitter fingers. Note that these results represent average measurements, while the previous graphs present the best measured results.

As mentioned previously, for each HBT V_{EB} was adjusted for maximum small-signal microwave gain, resulting in the optimal collector current density J_C^{opt}. For Wafer A, J_C^{opt} decreased from 2.5×10⁴ to 1.5×10⁴ A/cm² for emitter areas from 20 to 500 μm², respectively. Other than this slight area dependence, J_C^{opt} did not vary with emitter geometry. This indicates that the variation is not due to current crowding or surface recombination but rather is due to self-heating generated from the total power dissipated in the HBT. Also, the J_C^{opt} for HBTs on Wafer B was approximately one-half that for HBTs on Wafer A, probably due to a slightly lower collector doping. Since gain decreases dramatically after the onset of base push-out, J_C^{opt} must occur at a lower current density than base push-out. Lower collector doping causes base push-out at lower current levels, which lowers J_C^{opt}. The decrease in gain above J_C^{opt} also limits the large-signal current swing for Wafer B, which leads to worse power performance.

The DC large-signal current gain β for HBTs biased at J_C^{opt} was close to the maximum current gain for these HBTs, and it varied from 19.5 to 15.5. In general, β decreased with increasing emitter area but was independent of the emitter geometry, which can again be attributed to self-heating. For a fixed HBT size, Wafer B demonstrated greater β than Wafer A (between 5% and 45% greater, depending on bias). In Wafer B, the electric field generated by the doping gradient in the base pushes the injected holes towards the collector more rapidly, which reduces the number of holes that recombine. Simulations indicated that the dominant component of the base current is Auger recombination in the neutral base [1], so any decrease in base recombination results in significantly increased gain.

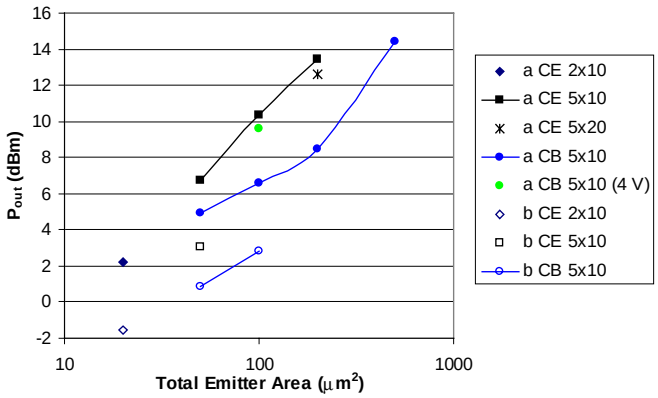

Fig. 4: Output power at 1-dB gain compression for HBTs biased at J_C^{opt}.

Variations in power performance can be seen in the output power at 1-dB of gain compression (P_o^{-1dB}, in Fig. 4) and in the maximum power-added efficiency (*PAE*) for HBTs biased at J_C^{opt}. Note that the tuning range of the load and source tuners limited the gain of the small and medium-to-large HBTs, respectively, and the maximum *PAE* typically occurred between the 2.5 and 3 dB gain compression points. In general, the P_o^{-1dB} scaled with the area of the HBT. Since the collector current also scaled with the HBT area, the *PAE* versus area is dominated by the HBT gain characteristics. The maximum *PAE* for common-emitter HBTs was 20% for the 2-finger 5×20 μm² HBT from Wafer A. The smaller bias current density and the 1- to 3-dB lower microwave gain of Wafer B contributed to its 4-dB lower P_o^{-1dB} and 7% lower *PAE*.

At the same V_{EC} bias, the P_o^{-1dB} is significantly (2 to 5 dB) higher for common-emitter HBTs than for common-base HBTs. This effect is primarily due to the limited output voltage swing imposed by V_{BC} = 3.2 V for the common-base HBTs. When V_{BC} was increased to 4.0 V (labeled "4 V" in the figure's legend), the P_o^{-1dB} increased to match the value for common-emitter HBTs. However, at either bias point, the microwave gain of the common-base HBTs is 3 to 6 dB higher than for the common-emitter HBTs. Since the *PAE* is essentially determined by the microwave gain and the gain compression characteristics, this leads to similar efficiency (17-18%) for both configurations when V_{BC} = 3.2 V and higher efficiency (22%) for common-base when V_{BC} = 4.0 V. In general, the *PAE* of the common-emitter HBTs was limited by low gain, and the *PAE* of the common-base HBTs was limited by early output power saturation. The *PAE* should be able to be increased by increasing V_{BC} in the common-base configuration. The values presented here are close to the *PAE* reported for GaAs-based PNP HBTs – 25% for common-base and 33% for common-emitter [3].

V. Discussion

The characteristics presented above give some insight to the limitations of power performance in PNP InP-based HBTs. In general, the power and efficiency performance is dominated by the microwave gain (or equivalently f_{max}) and the bias

conditions. For HBT designs that have their optimal f_{max} at higher J_C, the available output signal swing is larger, which increases P_o^{-1dB}. This implies that an increased collector doping (to delay base push-out) and an increased breakdown voltage are key elements to power performance. The higher gain and breakdown voltage for common-base HBTs clearly give a performance benefit over common-emitter HBTs. Typically, BV_{BC0} for common-base HBTs is twice that of BV_{ECO} for common-emitter HBTs, allowing for much higher bias voltages in the common-base configuration. When combining higher bias V_{BC} with its higher gain at frequencies close to f_T, common-base HBTs should be able to produce more output power at higher efficiencies than was presented.

Although the doping gradient in the base of Wafer B decreased the base transit time, the base resistance also increased, resulting in lower f_{max}, less high-frequency gain, and worse power performance than Wafer A. Increasing the base doping in Wafer B should decrease the base resistance while maintaining the improved f_T, which would increase f_{max} and the power performance.

Finally, since the high-frequency characteristics of these PNP HBTs were dominated by transit times rather than by parasitic charging times, their intrinsic power performance was only slightly dependent on device geometry or area. The lack of any significant gain or power dependence on the perimeter-to-area ratio indicates that surface recombination is not a major factor in these HBTs. However, the total device area still had a large influence on the input and output impedance of the HBT, making it difficult to fully match very small or very large HBTs.

Device modeling and analysis also suggested several potential improvements to the PNP HBT design for increased high-frequency power performance. In general, f_T was dominated by the base transit time, so either a doping gradient or a compositional gradient in the base can create an electric field to reduce the base transit time. Drift-diffusion simulations [1] indicated that removing the emitter-base spacer would reduce the base transit time while increasing the DC gain, since a significant number of holes recombine in the spacer. These modifications will cause an associated increase in f_{max} and in the gain at 10 GHz, which should significantly improve the X-band power performance and efficiency. Slightly increasing the base doping and thickening the collector will reduce R_BC_{BC}, which in turn will also increase f_{max}. Finally, the power-added efficiency was partially limited by the parasitic emitter and collector resistances, indicating that a thinner emitter cap and a thicker subcollector should be used.

VI. Conclusion

In this study, HBTs were fabricated and characterized to determine the power performance potential of PNP InAlAs/InGaAs HBTs. PNP HBTs demonstrated f_T and f_{max} as high as 13 and 35 GHz, respectively. Power performance at 10 GHz was comparable to InP-based NPN single HBTs, providing up to 0.49 mW/μm^2 of output power and a *PAE* of 24%. Although its graded base increase the f_T of HBTs on Wafer B, the base resistance also increased, causing a decrease in f_{max}, power performance, and efficiency. The HBT characteristics scaled well with area, which indicates that these devices are good candidates for power applications. Finally, common-base HBTs demonstrated up to 6 dB more gain while maintaining the same output power density as similar common-emitter HBTs at 10 GHz.

Acknowledgments

This work is supported by ARO MURI (DAAH04-96-1-0001).

References

[1] D. Sawdai, X. Zhang, D. Pavlidis, and P. Bhattacharya, "Performance Optimization of PNP InAlAs/InGaAs HBTs," *Proc IEEE/Cornell Conf on Advanced Concepts in High Speed Semiconductor Devices and Circuits*, pp. 269-277, 1997.

[2] S. Shi, K. P. Roenker, T. Kumar, M. M. Cahay, and W. Stanchina, "Simulation of PNP InAlAs/InGaAs Heterojunction Bipolar Transistors," *IEEE Trans. Electron Dev.*, Vol. 43, pp.1466-1467, September 1996.

[3] D. Hill, T.S. Kim, and H.Q. Tserng, "X-band Power AlGaAs/InGaAs P-n-p HBT's," *IEEE Electron Dev. Lett.*, Vol. 14, pp. 185-187, April 1993.

[4] K. Kobayashi, D. Umemoto, J. Velebir Jr., A. Oki, and D. Streit, "Integrated complementary HBT Microwave Push-Pull and Darlington Amplifiers with p-n-p Active Loads," *IEEE J. Solid-State Circuits*, Vol. 28, pp. 1011-1016, October 1993.

[5] L. M. Lunardi, S. Chandrasekhar, and R. A. Hamm, "High-Speed, High-Current-Gain P-n-p InP/InGaAs Heterojunction Bipolar Transistors," *IEEE Electron Dev. Lett.*, Vol. 14, pp. 19-21, January 1993.

[6] D. Slater, P. Enquist, J. Hutchby, A. Morris, and R. Trew, "Pnp HBT with 66 GHz f_{max}," *IEEE Electron Dev. Lett.*, Vol. 15, pp. 91-93, March 1994.

[7] D. Sawdai, K. Hong, A. Samelis, and D. Pavlidis, "High Power Performance InP/InGaAs Single HBTs," *22nd Int. Symp. Compound Semiconductors*, pp. 621-626, 1995.

[8] D. Sawdai, J-O Plouchart, D. Pavlidis, A. Samelis, and K. Hong, "Power Performance of InGaAs/InP Single HBTs," *8th Int Conf Indium Phosphide and Related Materials*, pp. 133-136, 1996.

[9] C. Nguyen, T. Liu, M. Chen, and R. Virk, "Bandgap Engineered InP-Based Power Double Heterojunction Bipolar Transistors," *9th Int Conf Indium Phosphide and Related Materials*, pp. 15-19, 1997.